I. KALEMBA*, S. DYMEK*, C. HAMILTON**, M. BLICHARSKI*

MICROSTRUCTURE EVOLUTION IN FRICTION STIR WELDED ALUMINIUM ALLOYS

MIKROSTRUKTURA POŁĄCZEŃ STOPÓW ALUMINIUM WYKONANYCH METODĄ ZGRZEWANIA TARCIOWEGO Z MIESZANIEM MATERIAŁU ZGRZEINY

Friction stir welding (FSW) is a relatively new technique which was invented by The Welding Institute in the early nineties. It is a very promising method of welding aluminum alloys on a large scale. FSW is a novel solid-state joining process that is gaining popularity in the manufacturing sector and, in particular, the aerospace industry. During the FSW process the material is mixed and undergoes intense plastic deformation accompanied by a temperature increase. This results in significant microstructural evolution, including change in grain size, grain boundary character, coarsening and dissolution of precipitates and their further re-precipitation. The objective of this study was to evaluate the microstructural changes produced by friction stir welding of age-hardenable aluminum alloys from the 6xxx and 7xxx series. This research also addresses microstructure correlation with basic mechanical properties. The microstructure of the weld was examined by light and electron microscopy. The particular regions, i.e. thermomechanically affected zone, heat affected zone and unaffected base material, were studied in detail to better understand the microstructural evolution during FSW in various aluminum alloys.
Keywords: friction stir welding, aluminum alloys, microstructure, mechanical properties

Zgrzewanie tarciowe z mieszaniem materiału zgrzeiny (ang. friction stir welding – FSW) jest jedną z nowych technologii spajania, która została opracowana w The Welding Institute w 1991 roku. Jest to bardzo obiecuj.ca technika łączenia stopów aluminium, która umożliwia ich stosowanie na szerszą skalę. W ostatnich latach znalazła ona szerokie praktyczne zastosowanie, szczególnie w przemyśle lotniczym. Proces zgrzewania tarciowego z mieszaniem materiału zgrzeiny zachodzi bez udziału fazy ciekłej, w odróżnieniu od metod konwencjonalnych. W procesie FSW materiał poddawany jest intensywnemu odkształceniu plastycznemu w podwyższonej temperaturze, czego wynikiem jest zmiana mikrostruktury. Obejmuje ona zmianę rozmiaru ziaren, charakteru granic ziaren, koagulację i rozpuszczanie cząstek oraz ich ponowne wydzielanie. Celem badań jest ocena mikrostruktury połączeń utwardzanych wydzieleniowo stopow aluminium z serii 6xxx i 7xxx wykonanych metodą FSW. Przeprowadzono rownież badania własności mechanicznych w celu korelacji ich z mikrostrukturą złącza. Badania mikrostruktury obejmowały mikroskopię świetlną i elektronową. W celu dokładniejszego zrozumienia zmian mikrostrukturalnych podczas procesu FSW w różnych stopach, obserwacji mikroskopowej poddano probki z charakterystycznych obszarow tj. środka zgrzeiny, strefy cieplno-plastycznej, strefy wpływu ciepła i materiału rodzimego.

1. Introduction

The development of new materials and their practical application constitute a great challenge for manufacturing sectors in many branches of industry. Numerous efforts concentrate on considerable reduction of manufacturing costs for various components and their assemblies. For this reason, novel manufacturing concepts are under continuous development. It is the joining technology that has made tremendous progress in the recent decade. The application of many new advanced materials is limited by the problems associated with their joining, and this problem also pertains to traditional metallic materials like aluminum alloys. Conventional joining technologies like fusion welding, brazing or riveting do not provide sufficient quality of joints especially in age-hardenable Al alloys.

* AGH UNIVERISTY OF SCIENCE AND TECHNOLOGY, FACULTY OF METALS ENGINEERING AND INDUSTRIAL COMPUTER SCIENCE, 30-059 KRAKÓW, 30 MICKIEWICZA AV., POLAND
** MIAMI UNIVERSITY, DEPARTMENT OF MECHANICAL AND MANUFACTURING ENGINEERING, OXFORD, OHIO, USA

One new joining technology is friction stir welding (FSW), which was developed in 1991 by The Welding Institute. Unlike traditional welding techniques, FSW is a solid-state joining process, whose basic concept is extremely simple [1]. A rotating tool with a specially designed pin is inserted between abutting edges of sheets to be joined and traversed along the line of the joint as shown in Figure 1 [2]. Friction between the tool and workpieces as well as severe plastic deformation increase the temperature in the materials to be joined. This localized heating together with a pressure exerted by the tool shoulder plasticize the material and stir it around the rotating and moving pin forming the weld [3]. The welded joint is fundamentally defect-free and displays superior mechanical properties compared to conventional fusion welds [3-6]. Since no melting occurs during FSW, the process is performed at much lower temperatures than conventional welding techniques and circumvents many of the environmental and safety issues associated with these methods.

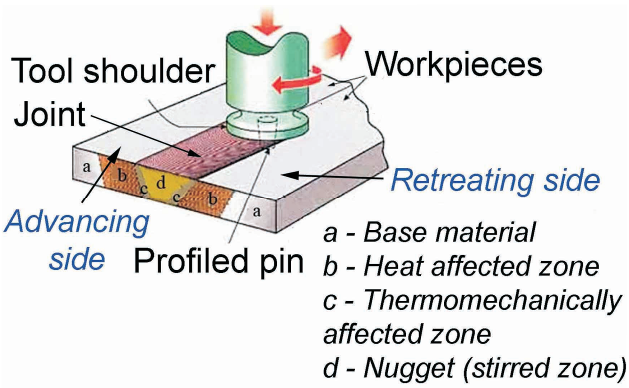

Fig. 1. Schematic illustration of the FSW process [2]

During the recent years, numerous investigations have been undertaken to characterize the principles of FSW and to model the microstructural development. The current status of FSW research has been well summarized by Mishra and Mahoney [3]. It is clear from their work that the microstructure and resulting properties produced during FSW of aluminum alloys are dependent on several factors. The contributing factors include alloy composition, alloy temper, welding parameters, thickness of the welded plates as well as the shape and geometry of applied tools. The changes in microstructure and properties in FSW joints differ in particular alloys. These changes are exceptionally evident in age-hardenable alloys where severe plastic deformation accompanied by mixing of material as well as heating and cooling cycles alters the microstructure (and thus properties) in a significant manner. This research aims to compare the microstructure and properties of friction stir welded Al alloys belonging to two different families of age-hardenable alloys: 6xxx and 7xxx series.

2. Experimental procedure

Two classes of aluminum alloys were investigated: 6xxx and 7xxx. The first class was represented by 6061 and 6101 alloys while the other one by the 7136 alloy. Before welding, the 6xxx alloys were aged to the T6 temper, i.e. solution treated and artificially aged to the peak strength, while the 7136 alloy was aged to the T76 temper, i.e. solution treated and overaged. The chemical compositions of these alloys are presented in Table 1.

TABLE 1
Nominal chemical composition of investigated alloys [wt %]

Alloy	Al	Mg	Si	Zn	Cu	Cr	Zr
6061	Bal.	0.8 – 1.2	0.4 – 0.8	0.25	0.15 – 0.40	0.04 – 0.35	–
6101	Bal.	0.35 – 0.8	0.3 – 0.7	0.10	0.10	0.03	–
7136	Bal.	1.8 – 2.5	max. 0.12	8.4 – 9.4	1.9 – 2.5	max. 0.05	0.10 – 0.20

The aluminum alloys were obtained as extrusions with a thickness of 6.35 mm and joined by the FSW method at the Edison Welding Institute in Columbus, Ohio. The joining parameters applied in the FSW tests are presented in Table 2. For the current research the 6xxx alloys were plated with Sn before welding.

TABLE 2
Welding parameters applied for the investigated alloys

Alloy	Applied load [kN]	Rotation speed [RPM]	Welding speed [mm/min]
6061	22.5	900	300
6101	22.5	900	300
7136	26.7	250	120

Microstructural investigation was performed by light (LM) and electron microscopy (scanning – SEM and transmission – TEM). For TEM examination thin foils were prepared from specific regions of the tested sample: base material, heat affected zone, thermomechanically affected zone and the center of the weld. The thin foils were excised from the plane perpendicular to the weld direction. For thin foil preparation, a solution of nitric acid/methanol (1:2) was used. Electropolishing was performed at a voltage of 12 V and a temperature of -30 °C. SEM investigation comprised analysis of images formed by back scattered electrons (BSE) and analysis of fracture surfaces by the use of secondary electrons.

To correlate the microstructural characteristics with the mechanical properties of the welds, tensile tests and hardness measurements were performed. Tensile samples were prepared from base and welded material. Tensile samples were excised from the welded material in such a way that the tensile axis was perpendicular to the weld seam. With this specimen orientation, the weld is centered along the tensile specimen, and as such, the load is applied transverse to the weld direction and across all microstructural regions associated with the welding process, i.e. the weld nugget, the heat affected zone (HAZ) and the thermomechanically affected zone (TMAZ) distinctive to FSW. The Vickers hardness profile of the welds was measured on the cross-section perpendicular to the welding direction at the 9.81 N load. The distance between sampling points was 1 mm.

3. Results and discussion

The microstructures of the 6061 and 6101 alloys were very similar and are described jointly without differentiating both alloys (referred to as the 6xxx alloys). The typical microstructures of the alloys in as-received conditions (base materials) are shown in Fig. 2a,b. Both microstructures are composed of a high density of hardening nano-sized precipitates.

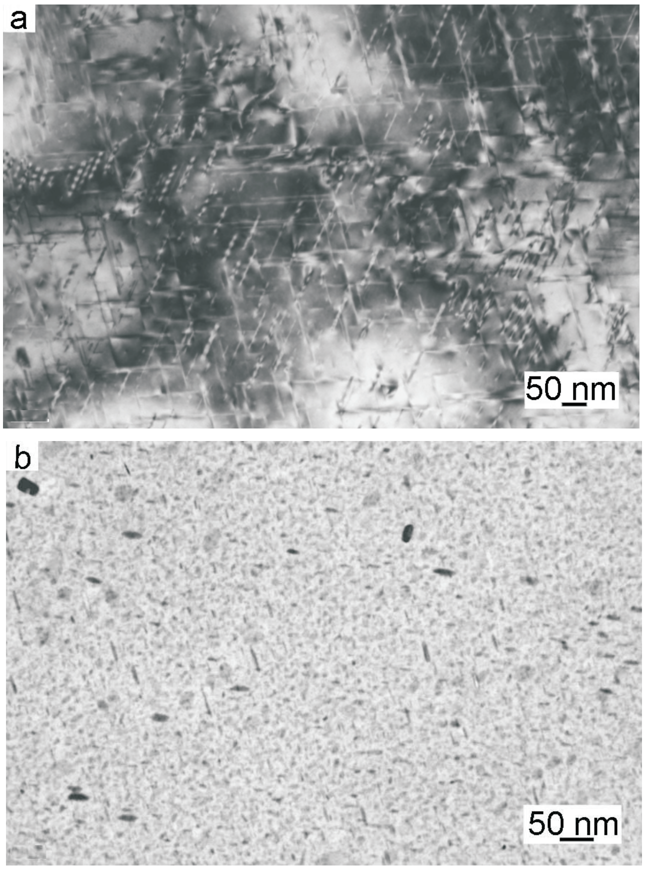

Fig. 2. Hardening precipitates in the base alloys, TEM: a) 6061-T6, b) 7136-T7

Fig. 3 shows microstructures of welds in the 6061 and 7136 extrusions revealed on cross-sections perpendicular to the weld seam at low magnification. There is a striking visual difference between appearance of these welds. The weld in the 7136 alloy is fairly uniform and does not show a characteristic "nugget" as observed in the 6xxx alloys. The well-defined nugget of the 6xxx alloys is characterized by an "onion ring" pattern, frequently found in other Al alloys joined by FSW [3,7,8]. The pronounced differences in weld microstructure result from the different welding parameters applied during the FSW process on the one hand and from the Sn flash on the 6xxx extrusion surfaces that was introduced to help visualize the material flow during FSW (Sn is almost nonsoluble in Al).

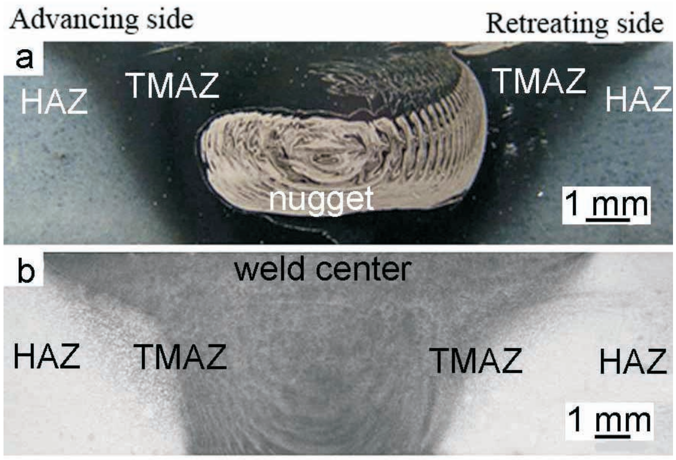

Fig. 3. Weld appearance at low magnification; LM: a) alloy 6061, b) alloy 7136

The origin of "onion rings" has not been fully explained to date, though some attempts have been undertaken. Some earlier works on FSW attempted to associate the occurrence of "onion rings" with the heat generated during the FSW process. Biallas et al. [9] indicated that the "onion ring" patterns are observed for "hot" welds rather than for "cold" ones. Indeed, Krishnan [10] explained the disappearance of the rings by an increase of temperature, i.e. when tool rotational speed is higher and welding speed slower. In the present investigation, the ratio of rotational speed to welding speed (taken as an indicator of the amount of generated heat) was higher for 6xxx than 7136 alloys and thus more heat generation is expected for the 6xxx alloys despite lower load. However, the occurrence of "onion rings" took place in the 6xxx alloys rather than the 7136 alloy. The likely reason for this might be the difference in strength between the alloys. The base metal with lower yield strength, lower hardness and higher ductility (6xxx) can be plastically deformed more easily compared to the base metal with high strength, high hardness and low ductility. Higher heat input may cause turbulent metal flow around the tool pin due to excess plasticization of base metal under the tool shoulder and thus promote less uniform microstructure of the weld, i.e. formation of "onion rings".

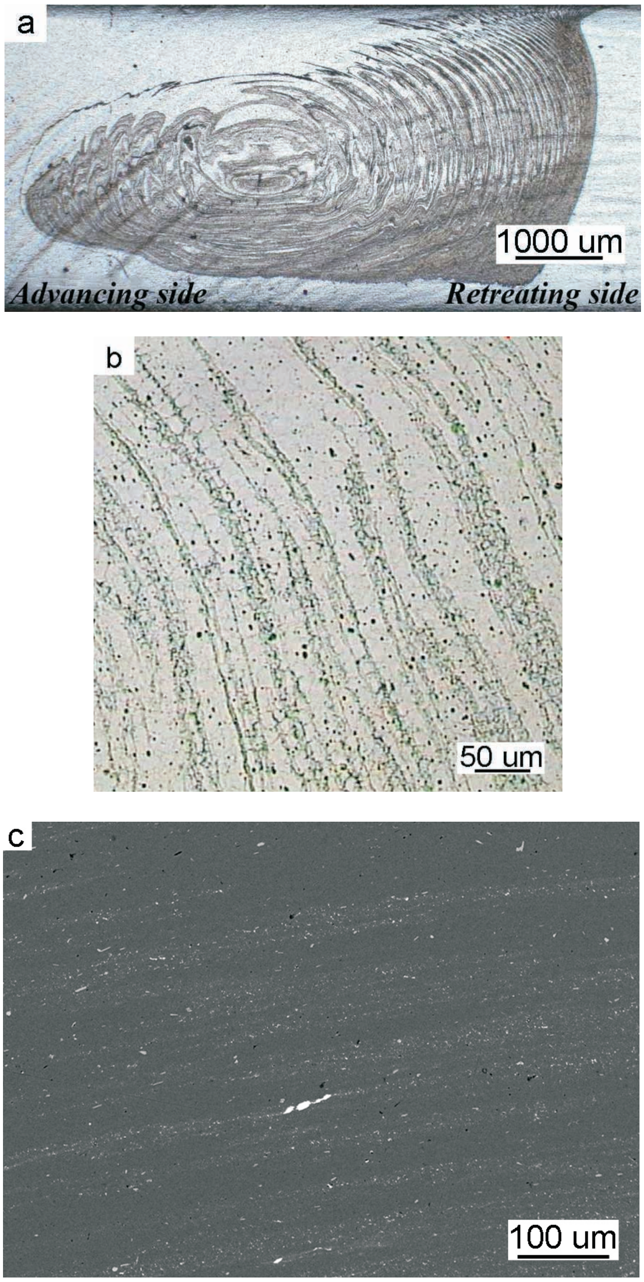

Fig. 4. Microstructure of the weld in 6101 alloy: a) nugget, LM, b) "onion rings", LM, c) "onion rings", SEM BSE

The present research gives new insight into the mechanism of "onion rings" formation. The complex flow pattern of the FSW process is clearly evident within the FSW nugget in 6xxx alloys which were plated with tin before the FSW process. The material flow is highlighted by the banded microstructure of the nugget (Fig. 4). The contrast between the two bands is associated with an uneven distribution of secondary phase particles. The "dark" bands reflect a high particle density while the "bright" ones represent areas with low particle density. The detailed study performed on 6xxx alloys with utilization of Z-contrast formed by backscattered electrons (BSE) in SEM revealed a banded structure formed by particles composed by elements with an atomic number Z higher than the Al atomic number (Fig. 4c). The chemical analysis of these particles showed the presence of Sn. Because tin is only present on the surface of the extrusions as plating, the unique occurrence of tin in the nugget is extremely important. It may indicate that the "onion rings" are formed by the material from the surface of the welded plates.

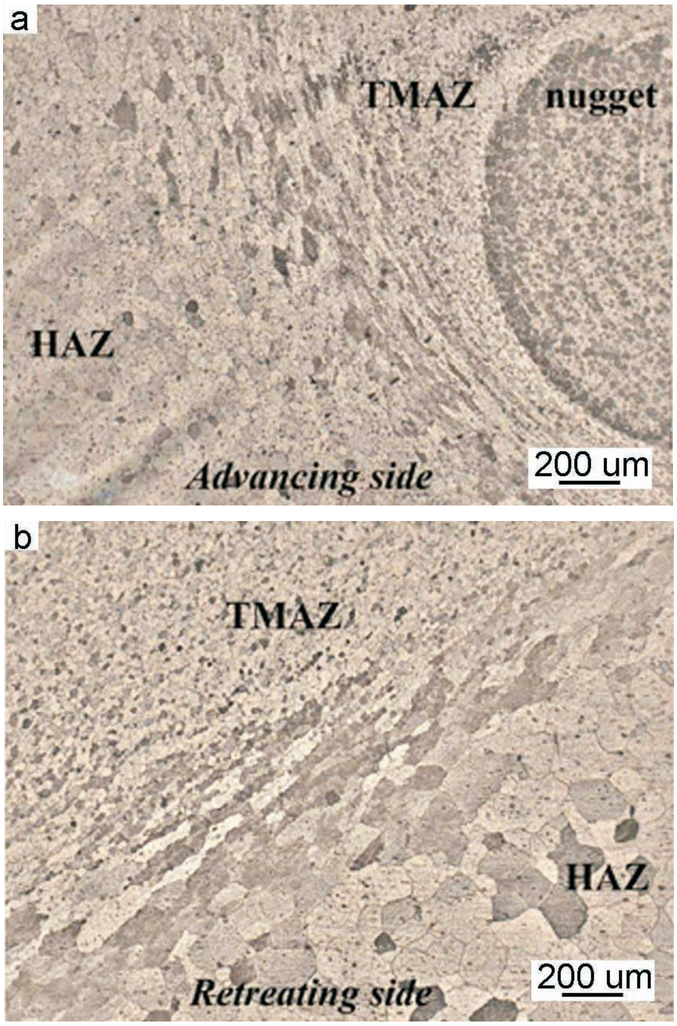

Fig. 5. Microstructure of FSW weld in 6061 alloy, LM: a) advancing side, b) retreating side; (HAZ – hest affected zone; TMAZ – thermomechanically affected zone)

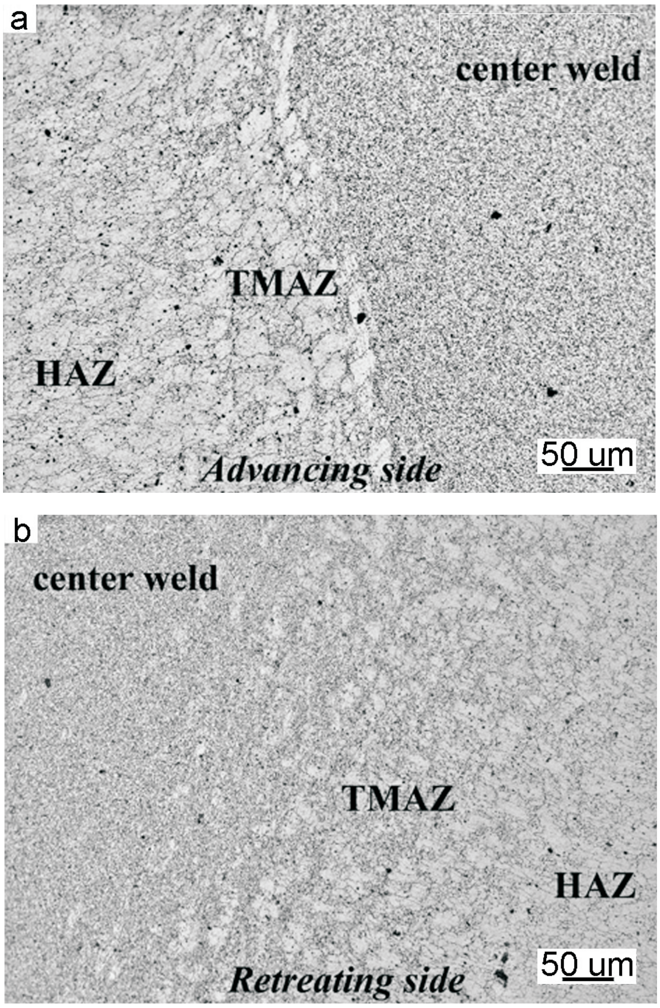

Fig. 6. Microstructure of FSW weld in 7136 alloy, LM: a) advancing side, b) retreating side

Another noteworthy feature, common for both alloy classes, is a noticeable difference between the microstructure of the weld boundaries on advancing and retreating sides. In the 6xxx alloys the borders between the nugget and its surrounding are always sharp. In the 7136 alloy, on the advancing side the boundary is sharp, and well-defined, whereas on the retreating side a gradual transition from the microstructure of the weld center to that of the base material occurs. The weld borders for both classes of alloys are illustrated in Fig 5 and 6. In the nugget or weld center (stir zone) the grains show little deformation or elongation in the flow direction, suggesting that full recrystallization has occurred. The grain size is approximately equivalent in both the "bright" and "dark" bands and varies between 10 μm and 20 μm. This observation differs from other studies of aluminum alloys under similar welding conditions [8,11]. In these investigations, the authors concluded that fine, equiaxed recrystallized grains comprised the dark bands, and coarse recrystallized grains comprised the lighter ones.

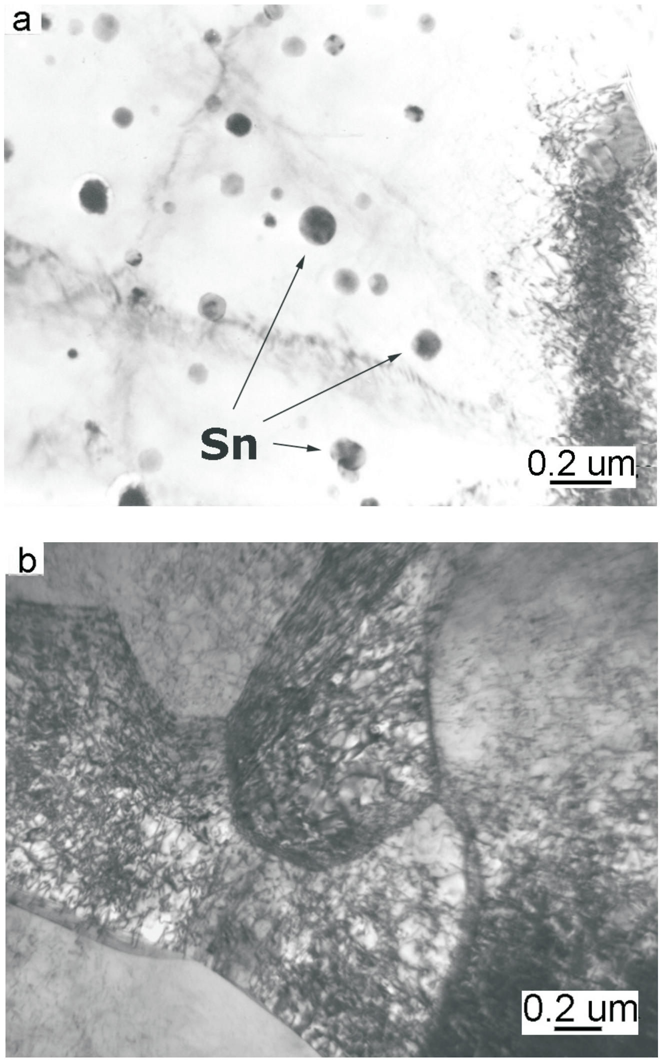

Fig. 7. TEM weld microstructure in 6061 alloy: a) nugget, arrows indicate Sn particles, b) TMAZ

Fig. 7 shows TEM micrographs of the nugget and TMAZ in the weld of the 6061 alloy. In the nugget (stir zone) Sn particles were revealed on TEM micrographs. However, neither in the TMAZ nor in the HAZ the tin particles were found. This finding confirms the SEM BSE observation that the material from the surface is extruded into weld center and forms the characteristic nugget. The microstructure of the TMAZ exhibited a relatively high dislocation density confirming significant dislocation activity within this zone. Fig. 8 shows the TEM weld microstructure in the 7136 alloy. The FSW process influences not only grain size, but also precipitate size. Precipitates in the weld center (Fig. 8a) no longer form typical hardening dispersoids; they are much larger than in the HAZ (Fig. 8b). In the HAZ, precipitate free zones are observed around the grain boundaries with large precipitates on the grain boundaries. In the weld center large precipitates, greater than 100 nm in diameter, as well as in the HAZ, identified as $MgZn_2$, were found.

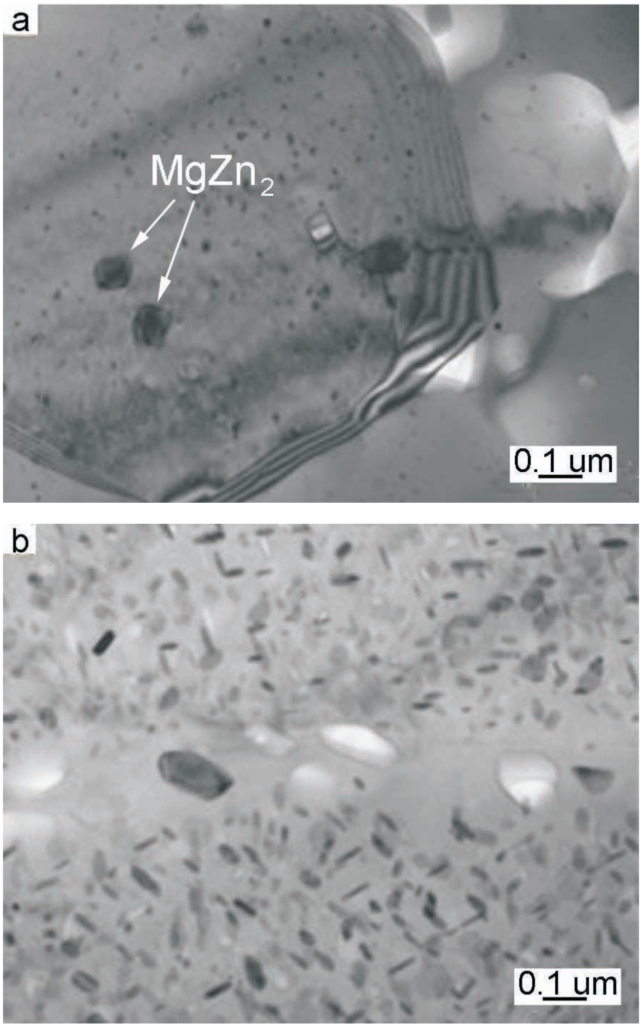

Fig. 8. TEM weld microstructure in 7136 alloy: a) weld center, b) HAZ

The changes in microstructure result from different thermomechanical history for particular regions. The weld center is subjected to severe plastic deformation combined with the physical flow of the material around the pin (stirring) and substantial increase of temperature. The hardening phase is destroyed in this region due to high temperature (thermal dissolution) and sequential cutting of coherent precipitates by gliding dislocations (mechanical dissolution). Dynamic recrystallization as well as re-precipitation of secondary phases takes place in this region forming a microstructure composed of fine equiaxed grains and large precipitates. The areas adjacent to the weld are subjected to plastic deformation, however, no material stirring takes place (thermomechanically affected zone — TMAZ). This zone is characterized by a gradient of accommodated strain and also gradient of temperature. This exerts an influence on microstructure – grains are elongated and their interiors are filled with dislocations. The hardening precipitates ripen and along grain boundaries precipitation free zones appear. The microstructure alters in a continuous way to the zone where plastic deformation is absent. Within this zone only a temperature gradient exists, and as such this zone is referred to as a HAZ. The temperature increase in this zone results in grain growth and coarsening of hardening precipitates. In the HAZ, precipitation free zones also form along grain boundaries.

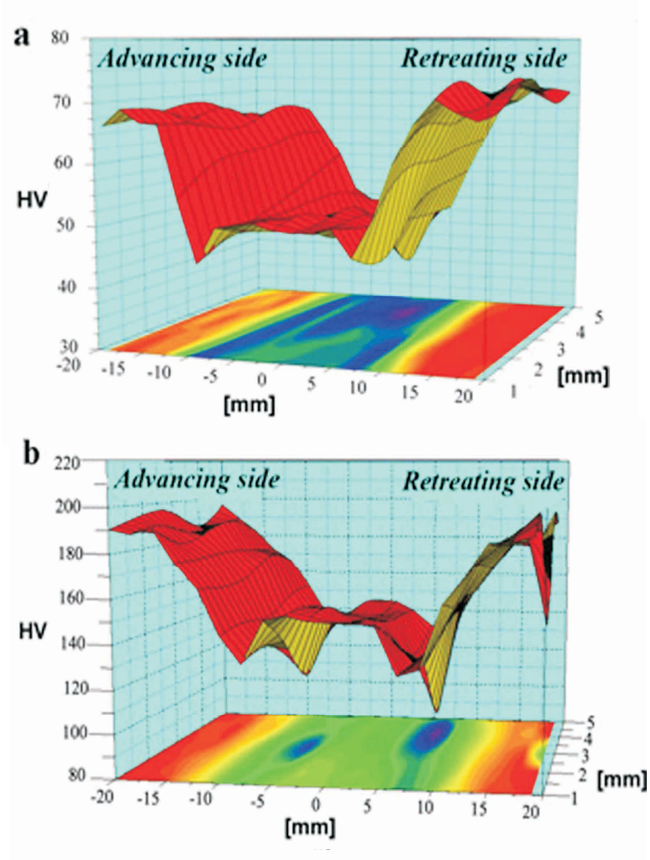

Fig. 9. Hardness profiles for as-welded samples: a) 6061 alloy, b) 7136 alloy

In the weld centers, all examined alloys had a fine-grained recrystallized structure. In the TMAZ, grains are larger and elongated since the extent of plastic deformation and temperature increase are less than that in the center weld. FSW also produces changes in microstructure within the HAZ; however, since this region does not undergo any plastic deformation and the temperature increase is lower, the changes are not so dramatic as in the nugget or TMAZ.

The changes in microstructure are reflected in the hardness profile across the weld (Fig. 9). Results of hardness tests are displayed in the map form. The 6xxx alloys had lower hardness compared to the 7136 alloy. The base material hardness of the 6xxx alloys averages 75 HV, while 7136 – 200 HV. Regardless of this the weld of each alloy exhibits lower hardness than the base material. Hardness of weld decreases by about 30%. Hardness profiles displayed the lowest hardness at the interface between HAZ and TMAZ, especially on the retreating side. In the case of the 7136 weld the hardness decreases in this region by approximately 45%. This observation is consistent with the mechanical properties and the consistent failure of the test coupons on the retreating side. The other mechanical properties are summarized in Table 3. The welded specimens have lower mechanical properties compared to the base materials. For example, in 6061-T6 alloy case, the yield and ultimate tensile strengths decreased by approximately 47% and 21%, respectively, from base material. Also elongation was lower than the base material.

TABLE 3

Mechanical properties of the tested alloys

Material	Yield Strength $R_{0,2}$ [MPa]	Tensile Strength, R_m[MPa]	Elongation, ε [%]
Base 6101-T6	174	200	9.4
Weld 6101-T6	69	130	3.4
Base 6061-T6	159	194	12.3
Weld 6061-T6	84	153	7.8
Base 7136-T7	607	634	11
Weld 7136-T7	386	476	6

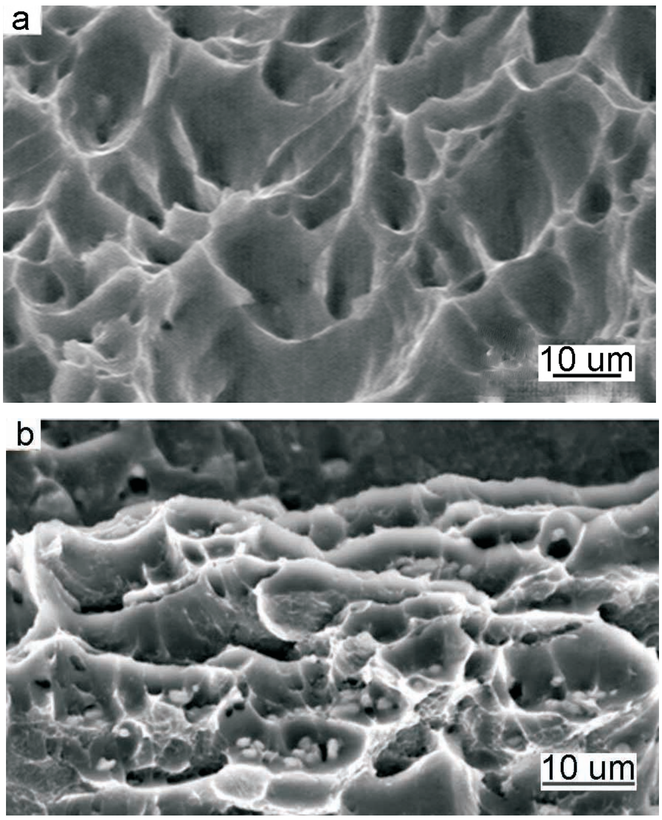

Fig. 10. Typical fracture surfaces, SEM: a) 6101 alloy, b) 7136 alloy

Figure 10 contains SEM micrographs of representative FSW welded fracture surfaces of the 6xxx and 7136 alloys. Fracture surfaces of tensile coupons from all tested material displayed ductile rupture. It is of particular interest to note that fracture of all FSW tensile samples consistently occurred on the retreating side of the weld along the interface between the heat affected zone and thermomechanically affected zone, approximately 10 mm from the center. Tensile failure on the retreating side is a common phenomenon, which was reported in research studies on aluminum alloys [8,11].

4. Conclusions

1. The FSW joints of all tested alloys exhibit diverse types of microstructure resulting from a complex thermomechanical history of particular weld zones. The weld nugget produced during FSW of the 6xxx alloys exhibited a banded microstructure consisting of alternating layers of material "rich" in Sn particles and material "poor" in the particles. The TMAZ, HAZ and base material did not indicate any Sn-containing phases. Since tin is only present on the surface of the extrusions, the Sn-rich bands represent surface material that has flowed into the nugget region. The "onion ring" structure is thus formed by the alternating layers of the material from the surface and from within the thickness of the welded extrusions.
2. The FSW process applied to the 7136 alloy did not produce any "onion ring" structure.
3. The weld centers of all alloys exhibited a microstructure composed of fine and recrystallized grains. The hardening precipitates are no longer present in the weld centers. Instead, coarse particles of equilibrium phases were found.
4. The welded materials have lower yield stress, tensile strength and hardness compared to the base materials. Retreating weld side shows the lowest mechanical properties. For all tested welds, fracture surfaces revealed typical ductile rupture.

Acknowledgements

The authors acknowledge the Polish Ministry of Science and Higher Education (Grant No. N50709432/2648) for their support of this research.

REFERENCES

[1] W. M. Thomas, Great Britain Patent Application No. 9125978.8, December 1991.

[2] http://www.twi.co.uk/j32k/unprotected/band_1/fswintro.html

[3] R. S. Mishra, M. W. Mahoney, Friction Stir Welding and Processing, ASM International, Ohio, USA, p. 1 (2007).

[4] M. A. Sutton, B. C. Yang, A. P. Reynolds, J. H. Yan, Mat. Sci. Eng. A **364**, 66 (2004).

[5] H. Hori, H. Tanikawa, N. Seo, K. Namba, Proc. of the 6th Int. Symp. on Friction Stir Welding, Montreal, Canada, October 10-13, (2007).

[6] R. M. Leal, A. Loureiro, Mat. Sci. Forum **514-516**, 697 (2006).

[7] M. A. Sutton, B. C. Yang, A. P. Reynolds, R. Taylor, Mat. Sci. Eng. **A323**, 160 (2002).

[8] Y. S. Sato, S. H. C. Park, H. Konawa, Metall. Mater. Trans. **A32**, 3023 (2001).

[9] G. Biallas, R. Braun, C. Dalle Donne, G. Staniek, W. A. Kaysser, Proc. of 1st Int. Symp. on Friction Stir Welding, Thousand Oaks, CA, USA, (1999).

[10] K. N. Kirshnan, Mat. Sci. Eng. **327A**, 246 (2002).

[11] M. W. Mahoney, C. G. Rhodes, J. G. Flintoff, R. A. Spurling, W. H. Bingel, Metall. Mater. Trans. **A29**, 1955 (1998).

Received: 20 December 2009.